Alternative NADH dehydrogenase (NDH2): intermembrane-space-facing counterpart of mitochondrial complex I in the procyclic *Trypanosoma brucei*

ZDENĚK VERNER[1,2,3], INGRID ŠKODOVÁ[1,3], SIMONA POLÁKOVÁ[4], VLADISLAVA ĎURIŠOVÁ-BENKOVIČOVÁ[3]†, ANTON HORVÁTH[3] *and* JULIUS LUKEŠ[1,2]*

[1] *Biology Centre, Institute of Parasitology, Czech Academy of Sciences, České Budějovice (Budweis), Czech Republic*
[2] *Faculty of Sciences, University of South Bohemia, České Budějovice (Budweis), Czech Republic*
[3] *Department of Biochemistry, Comenius University, Bratislava, Slovakia*
[4] *Department of Zoology, DAPHNE ČR – Institute of Applied Ecology, České Budějovice (Budweis), Czech Republic*

(*Received 3 July 2012; revised 7 August and 3 September 2012; accepted 5 September 2012; first published online 30 October 2012*)

SUMMARY

The respiratory chain of the procyclic stage of *Trypanosoma brucei* contains the standard complexes I through IV, as well as several alternative enzymes contributing to electron flow. In this work, we studied the function of an alternative NADH : ubiquinone oxidoreductase (NDH2). Depletion of target mRNA was achieved using RNA interference (RNAi). In the non-induced and RNAi-induced cell growth, membrane potential change, alteration in production of reactive oxygen species, overall respiration, enzymatic activities of complexes I, III and/or IV and distribution of NADH : ubiquinone oxidoreductase activities in glycerol gradient fractions were measured. Finally, respiration using different substrates was tested on digitonin-permeabilized cells. The induced RNAi cell line exhibited slower growth, decreased mitochondrial membrane potential and lower sensitivity of respiration to inhibitors. Mitochondrial glycerol-3-phosphate dehydrogenase was the only enzymatic activity that has significantly changed in the interfered cells. This elevation as well as a decrease of respiration using NADH was confirmed on digitonin-permeabilized cells. The data presented here together with previously published findings on complex I led us to propose that NDH2 is the major NADH : ubiquinone oxidoreductase responsible for cytosolic and not for mitochondrial NAD^+ regeneration in the mitochondrion of procyclic *T. brucei*.

Key words: *Trypanosoma*, mitochondrion, dehydrogenase, respiration, NDH2.

INTRODUCTION

Trypanosoma brucei is a unicellular parasite that causes sleeping sickness in humans and nagana in cattle. Due to its detrimental effect on the rearing of cattle, the veterinary disease renders vast areas of sub-Saharan Africa unsuitable for agriculture. During its life cycle, *T. brucei* faces 2 dramatically distinct environments: the bloodstream of its mammalian host and the midgut and salivary glands of its tse-tse fly vector *Glossina* spp. While the blood is an environment with a constant level of glucose, the insect represents a glucose-poor environment. These environmental differences are reflected in major changes of the mitochondrion. In the bloodstream stage, the mitochondrion is represented by a reduced tubular organelle lacking a typical respiratory chain (Clarkson *et al*. 1989). This stage meets its ATP demands purely by glycolysis and excretes pyruvate as the major end-product. In contrast, in the procyclic stage the mitochondrion contains all the classical respiratory complexes and oxidative phosphorylation, contributing substantially to ATP production (for a recent review see Tielens and van Hellemond, 2009).

A classical electron transfer chain consists of 4 multisubunit complexes: NADH : ubiquinone (NADH:Q) oxidoreductase (complex I), succinate dehydrogenase (complex II), cytochrome *c* reductase (complex III) and cytochrome *c* oxidase (complex IV). Along with these large multi-subunit complexes, several single-subunit enzymes that contribute to the flow of electrons are known in the trypanosome mitochondrion. In the case of *T. brucei*, such representatives are glycerol-3-phosphate dehydrogenase (G3PDH) (Guerra *et al*. 2006), alternative rotenone-insensitive NADH:Q oxidoreductase (NDH2) (Fang and Beattie, 2002) and trypanosome alternative oxidase (TAO) (Chaudhuri *et al*. 1995). TAO mediates terminal transfer of electrons to oxygenproducing water, whereas the other 2 enzymes supply electrons to ubiquinone. While complexes III and IV, and also complex I in other eukaryotes, pump protons out of the mitochondrial matrix, none of the

* Corresponding author: Biology Centre, Institute of Parasitology, Branišovská 31, 370 05 České Budějovice, Czech Republic. Tel: +420 387 775 416. Fax: +420 385 310 388. E-mail: jula@paru.cas.cz
† Current address: Berlin Chemie AG, Bratislava, Slovakia.

Parasitology (2013), **140**, 328–337.
doi:10.1017/S003118201200162X

known single-protein enzymes is capable of such activity.

In *T. brucei*, all respiratory complexes have been studied to some extent. Complex I was shown to be present in both the procyclic and bloodstream stages. However, RNAi-based depletion of 3 of its core subunits in the procyclic stage did not affect viability of cells grown in media either containing or lacking glucose (Verner *et al*. 2011). Null mutants for 2 core subunits of complex I generated in the bloodstream stage showed a similar lack of an observable phenotype (Surve *et al*. 2011). Complex II can be disrupted in a glucose-containing medium without any effect on the growth of the procyclic cells, although in a medium depleted for glucose, disruption of this complex is lethal (Coustou *et al*. 2008). Finally, complexes III and IV were shown to be essential for growth and maintenance of mitochondrial membrane potential in the procyclic trypanosomes even on glucose (Horváth *et al*. 2005). Recent analysis of cells RNAi-depleted of 3 novel subunits of complex IV revealed disparate phenotypes, particularly regarding the activity of complex III (Gnipová *et al*. 2012).

The non-essentiality of any of the tested core subunits of complex I had led to the hypothesis that its activity can be fully replaced by NDH2. This flavin-containing enzyme (Fang and Beattie, 2002) was upon overexpression in and purification from bacteria able to perform NADH:Q reaction with Q0, Q1 and duroquinone as acceptors *in vitro*. Furthermore, the enzyme was shown to be capable of utilizing deamino NADH and NADPH as substrates *in vitro* (Fang and Beattie, 2003). We have shown previously that diphenylene iodonium (DPI), an inhibitor of flavin enzymes, was a specific inhibitor of NDH2 in *Phytomonas serpens*, a kinetoplastid flagellate closely related to *T. brucei* (Čermáková *et al*. 2007). Mitochondria of the procyclic *T. brucei* depleted for subunits of complex I showed an increased sensitivity of the NADH : ubiquione-2 (Q2) activity to DPI, which was mirrored by a lower sensitivity to rotenone, a specific inhibitor of complex I (Verner *et al*. 2011). The properties of NDH2 established by Fang and Beattie (2003) together with data obtained from studies of complex I (Surve *et al*. 2011; Verner *et al*. 2011) supported our hypothesis that in the mitochondrion of *T. brucei* NDH2 might preferentially be used for NAD^+ regeneration.

To investigate the putative ability of NDH2 to fully compensate for the loss of complex I, we have herein subjected *NDH2* to gene silencing using tetracycline-inducible RNAi. Our results indicate that NDH2 is facing intermembrane space, rendering complex I responsible only for the regeneration of matrix NAD^+. Moreover, NDH2 is essential for the maintenance of mitochondrial membrane potential in procyclic *T. brucei*.

MATERIALS AND METHODS

Cloning and Northern blot analysis

A 593 bp-long fragment of the NDH2 gene (Tb927.10.9440) was PCR-amplified using primers N2-fw (5′-GGATCCGACCCTCACCACTA-3′) and N2-rv (5′-CAAGCTTGCGGGTAAGTCCAC-3′) (added *Bam*HI and *Hin*dIII restriction sites are underlined). The amplicon was cloned into the pGEM®-T-Easy vector (Promega), sequenced, excised via the above restriction sites and recloned into the p2T7–177 RNAi vector (Wickstead *et al*. 2002).

Total RNA was isolated using either TRI Reagent® (Sigma) or High Pure RNA Isolation Kit (Roche). Northern blot analysis was performed with the NDH2 gene fragment used as a probe. Hybridization took place overnight at 55 °C in Na-Pi solution (Vondrušková *et al*. 2005) and was followed by a 2-step wash (2 × SSC +0·1% SDS for 30 min at room temperature and 0·2 × SSC +0·1% SDS for 30 min at 55 °C). Results were visualized using Typhoon 9410 (Amersham Biosciences).

Parasite cultivation, transfection and induction

Strain 29–13 of procyclic *T. brucei* was grown in SDM-79 supplemented with 10% FBS, hygromycin (50 μg/ml) and G418 (15 μg/ml). NotI-linearized RNAi constructs were electroporated as described previously (Hashimi *et al*. 2008), cells were selected using phleomycin (2·5 μg/ml) and diluted 10x upon reaching a concentration of 10^7 cells/ml. For double stranded (ds) RNA production, cells were induced by the addition of tetracycline (1 μg/ml). For growth analysis, 3 parallel independent induced and non-induced cell lines were daily diluted to a starting concentration of 3×10^6 cells/ml and their growth was measured using the Z2 Particle Count and Size Analyzer (Beckman Coulter). Data were processed using Microsoft Excel, evaluations by Mann-Whitney U-test were perfomed using an on-line application (http://elegans.som.vcu.edu/~leon/stats/utest.html). Growth rates were evaluated using ANOVA for repeated measurements with post-hoc Tukey test by StatSoft STATISTICA 10.

Flow cytometry

Flow cytometry was performed using BD FACSCanto™ II and analysed by BD FACSDiva software. Subsequent calculations were performed in Microsoft Excel. Statistical evaluations were perfomed as described above. For each experiment, 3 parallel independent RNAi inductions were performed.

For measurement of mitochondrial membrane potential, cells were incubated for 20 min with

https://doi.org/10.1017/S003118201200162X Published online by Cambridge University Press

250 nM tetramethylrhodamide ethyl ester perchlorate (TMRE; Invitrogen), a cationic dye that is sequestered to the mitochondrion based on its membrane potential. As a negative control, cells were incubated with TMRE together with 50 μM carbonyl cyanide 4-(trifluoromethoxy) phenylhydrazone (FCCP, Sigma-Aldrich). Measurements of reactive oxygen species (ROS) production were performed by incubating the flagellates for 20 min with 1 mg/ml dihydrorhodamide 123 (DHR; Sigma-Aldrich). DHR is an uncharged non-fluorescent dye that passively difuses into the cells, where it is oxidized by ROS to fluorescent rhodamide 123. As a positive control, cells were incubated with DHR in the presence of 10 μM hydrogen peroxide (Sigma-Aldrich).

The machine was set up using untreated non-induced cells. In every measurement, 20 000 particles were recorded using a low flow rate. Forward- and side-scatter peaks were postitioned to 50. Autofluorescence at the FITC channel that was used for monitoring of DHR was set up to peak at approximately 100. Autofluorescence at the PE channel used for monitoring TMRE was set up to peak at approximately 600. Both axes were logarithmic.

For calculations, median values of fluorescence from total recorded particles in a given channel were used. Mitochondrial membrane potential was considered 100% in the non-induced cells stained with TMRE and 0% in TMRE-stained cells in the presence of uncoupler FCCP. Increase/decrease in the RNAi-induced cells was calculated as a fraction.

$(TMRE_{ind}\text{-}[TMRE + FCCP]_{ind})/(TMRE_{non}\text{-}[TMRE + FCCP]_{non})$. ROS production in the presence of DHR and H_2O_2 was considered as 100%. The production was then calculated as a fraction (DHR-Autofluorescence)/([DHR + H_2O_2]-Autofluorescence) × 100%. For both mitochondrial membrane potential and ROS production mean and standard deviation were calculated.

Enzymatic assays, glycerol gradient sedimentation and respiration

NADH:Q2 oxidoreductase activity and glycerol gradient sedimentation were performed as described previously (Verner *et al*. 2011). Succinate dehydrogenase, cytochrome *c* reductase and cytochrome *c* oxidase were measured as described elsewhere (Horváth *et al*. 2005).

For the measurement of G3PDH activity, the following reaction mixture was prepared: 75 μg of mitochondrial proteins were added to a 1 ml cuvette containing 50 mM Tris-buffer (pH 7·0), 0·15 mM 2,6-dichloroindophenol and 0·2 mM phenazine methosulfate. Activity was measured by recording the decrease of absorbance at 600 nm triggered by the addition of 50 mM DL-glycerol-3-phosphate.

For respiration of intact cells, approximately 2×10^7 cells were collected by centrifugation, re-suspended in fresh SDM-79 medium and their oxygen consumption was measured using a Clark electrode as described elsewhere (Horváth *et al*. 2005). After a 2 min stabilization, cyanide (KCN) and salicylhydroxamic acid (SHAM) were added. In an alternative experiment, the drugs were added in a reverse order. The cells were incubated for 2 min with each drug.

For respiration measurements of digitonin-permeabilized cells, procyclics from 70 ml of log-phase culture were pelleted (1000 ***g*** for 10 min at room temperature [RT]) and washed in manitol buffer (0·65 M manitol, 10 mM Tris, 40 mM KPi pH 6·8) at RT. Upon centrifugation under the same conditions, the pellet was re-suspended to a concentration of 10^8 cells/ml in manitol buffer supplemented with digitonin (150 μg in water/ml of buffer), inverted 4–6 times and incubated on ice for 5 min. Next, the mixture was centrifuged (1500 ***g*** for 3 min at 4 °C) and the resulting pellet was resuspended in respiration buffer (0·65 M manitol, 10 mM Tris, 40 mM KPi pH 6·8, 10 mM $MgSO_4$, 2·5 mg/ml BSA FAs free, 1 mM ADP). The mixture was kept on ice and a 750 μl aliquot was warmed to 27 °C for 10 min prior to the measurement. Then, an aliquot was placed inside the closed respiratory cell maintained at 27 °C. Upon stabilization, basal oxygen consumption was recorded for 4 min. Then, substrates (50 mM DL-glycerol-3-phosphate in 10 mM Tris-HCl pH 7·4, 20 mM succinate, 10 mM NADH, 20 mM 2-oxoglutarate, 20 mM pyruvate and 20 mM malate all in water) were added (maximum 10% of the total volume) and respiration was recorded for 2–4 min. Next, inhibitors were added (2·5 mM SHAM and 2·5 nM antimycin A both in ethanol, 100 μM DPI in methanol, 1 mM KCN and 20 mM malonate both in water; maximum 1% of the total volume) and respiration was recorded for an additional 2–4 min.

RESULTS

NDH2 supports growth of T. brucei procyclics

Upon selection of phleomycin-resistant cells, total RNA was isolated from the parental 29–13 cells, non-induced cells and those in which RNAi was induced for 3 days by the addition of tetracyclin (tet+) into the medium. Northern blot analysis was performed with the NDH2 gene fragment as a probe. Massive production of dsRNA followed by efficient elimination of the target mRNA proved that RNAi was successful. Following this experiment, the culture was diluted to a concentration 10 cells/ml and distributed into a 96-well plate to generate clones. Six of these were screened by Northern blot analysis and the clone labelled N2D1 was selected for further

https://doi.org/10.1017/S003118201200162X Published online by Cambridge University Press

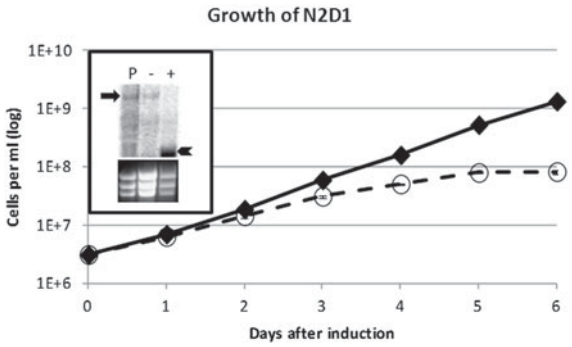

Fig. 1. Growth phenotype of procyclic *Trypanosoma brucei* interfered against NDH2. Growth curves of RNAi cell lines. Full and dashed lines correspond to the non-induced (tet −) and RNAi-induced (tet +) cells, respectively. *x* axis – days after induction; *y* axis – cell concentration/ml (log scale). The upper panel of the inset shows Northern blot analysis of the total RNA extracted from parental 29–13 cells (P), non-induced cells (−) and respective RNAi-induced cells (+). In the lower panel, the same gel was stained with ethidium bromide to visualize rRNA bands as a loading control. Arrow and arrowhead indicate NDH2 mRNA and double stranded RNA, respectively. A growth curve represents the mean of three independent parallel experiments. For detailed growth analysis see Supplementary Online resource 1.

experiments due to efficient ablation of the NDH2 mRNA (Fig. 1; inset).

Growth of this clone in the absence (tet −) and presence of tetracycline (tet +) was followed for 6 days (Fig. 1). The culture was daily diluted to a concentration 3×10^6 cells/ml, and the growth curve was plotted as a cumulative concentration against time. The ratio between induced and non-induced cell lines was computed for raw numbers as well as for growth rates (Supplementary Online resource 1). Since growth inhibition in the RNAi-induced cells compared to the non-induced ones started to appear on day 3 (approximately 50% slower growth), all the following experiments were performed on day 4. While the tet + cells exhibited retarded growth throughout the time-course, the cells remained viable even 6 days after induction.

Ablation of NDH2 leads to decrease of mitochondrial membrane potential

NDH2 is a part of the respiratory chain that does not pump protons across the inner membrane. Complex I competes with NDH2 for the same electron source (NADH) and electron acceptor ubiquinone (Q), with complexes III and IV being downstream. Thus, we tested the influence of the NDH2 ablation on mitochondrial membrane potential. Three independent parallel RNAi knock-down cell lines as well as non-induced controls were stained with TMRE and analysed by flow cytometry. A comparison

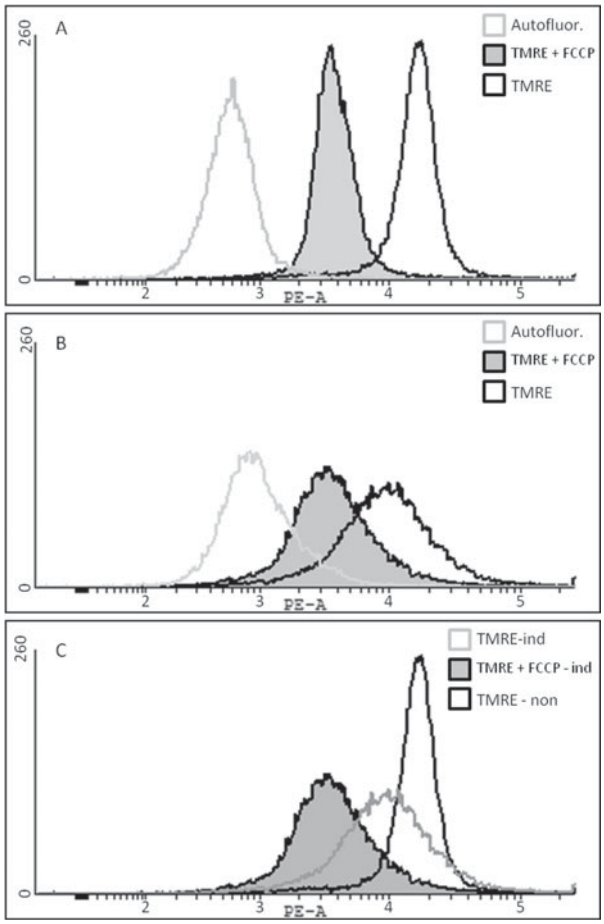

Fig. 2. Mitochondrial membrane potential is altered in NDH2 knock-down. Mitochondrial membrane potential was measured by flow cytometry following incubation of cells with 250 nM tetramethylrodamine ethyl ester (TMRE) alone or with 250 nM TMRE and 50 μM carbonyl cyanide 4-(trifluoromethoxy) phenylhydrazone (FCCP) 4 days after induction. Staining took place for 20 min. Fluorescence distribution plotted as a histogram. *x* axis – log scale of fluorescence; *y* axis – number of events. A representative experiment is shown. For full analysis see Supplementary Online resource 3. (A) Membrane potential of the non-induced cells: grey line: autofluorescence of the cells; black line: fluorescence of TMRE-stained cells; black line with grey filling: fluorescence of TMRE-stained cells in the presence of FCCP. (B) Membrane potential of the induced cells: grey line: autofluorescence of the cells; black line: fluorescence of TMRE-stained cells; black line with grey filling: fluorescence of TMRE-stained cells in presence of FCCP. (C) Overlay representing peaks used for mitochondrial membrane potential decrease calculation – see Supplementary Online resource 3: grey line: fluorescence of TMRE-stained induced cells; black line: fluorescence of TMRE-stained non-induced cells (100% mitochondrial membrane potential); black line with grey filling: fluorescence of TMRE-stained induced cells in presence of FCCP (0% mitochondrial membrane potential).

between the two populations showed a shift towards lower potential in the NDH2-silenced cells (Fig. 2). Quantitation using the uncoupler FCCP showed

https://doi.org/10.1017/S003118201200162X Published online by Cambridge University Press

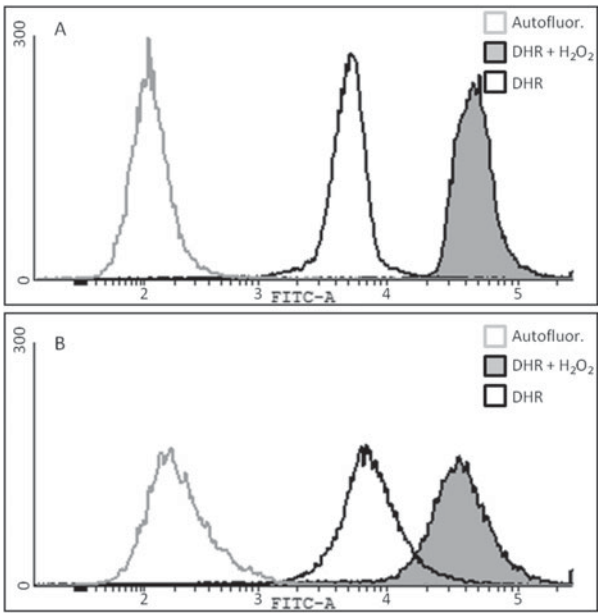

Fig. 3. Production of ROS is unaltered upon RNAi of NDH2. The production of reactive oxygen species was measured by flow cytometry following incubation of cells with 5 mg/ml dihydrorhodamide123 (DHR) alone or with 10 μM H_2O_2 and 5 mg/ml DHR 4 days after induction. The staining took place for 20 min. Fluorescence distribution plotted as a frequency histogram. *x* axis: log scale of fluorescence; *y* axis: number of events. A representative experiment is shown. For full analysis see Supplementary Online resource 4. Grey line: autofluorescence of the cells; black line: fluorescence of DHR-stained cells; black line with grey filling: fluorescence of DHR-stained cells with hydrogen peroxide (H_2O_2). (A) ROS production of the non-induced cells; (B) ROS production of induced cells.

a decrease of 51 ± 3% (Supplementary Online resource 2).

Respiratory complexes I and III are reported to be places of high reactive oxygen species (ROS) production (Galkin and Brandt, 2005; Ott *et al*. 2007). To test whether in the NDH2-depleted procyclic cells, complex I is active without contributing to the mitochondrial membrane potential, the level of ROS was assayed using dihydroethidium. We speculated that a higher electron flux through complex I would result in a higher leak to oxygen and consequently higher ROS. However, ROS production was unaffected in the RNAi-induced cells (Fig. 3; Supplementary Online resource 3).

Respiratory chain enzymes are altered in NDH2 knock-down cells

To follow the direct influence of NDH2 on the respiratory chain, the overall NADH:Q2 oxidoreductase activity was measured. In the NDH2-depleted cell line this activity was not significantly changed (Table 1). To confirm that the respiratory chain was indeed altered in these cells, *in vitro* activities of complexes II, III, IV and mitochondrial G3PDH were also measured. Comparison of the activities obtained from the non-induced and RNAi-induced cells revealed a significant increase of the G3PDH activity in the latter cells; however, the enzyme activities of the other enzymes did not exhibit a significant change (Table 1).

Table 1. Activities of respiratory enzymes in the non-induced and RNAi-induced NDH2 knock-down cells

(Enzyme: measured enzymatic activity (NADHQ2 – NADH: ubiquinone-2 oxidoreductase; complex II/SDH – succinate dehydrogenase; complex III/bc1 – cytochrome *c* reductase; complex IV/COX – cytochrome *c* oxidase; G3PDH – mitochondrial glycerol-3-phosphate dehydrogenase). Cells: Non, non-induced cells; Ind, RNAi-induced cells. Specific activity: average value ± standard deviation. n, number of measurements. *P*-value, significance level reached in *t*-test with $\alpha = 0{\cdot}05$. Enzymatic activities corresponding to 1 U catalyse the following changes: 1 nmol NADH/min (NADH:Q2), 1 nmol DPIP/min (SDH), 1 μmol cyt c/min (bc1 and COX) and 1 μmol DPIP/min (G3PDH). * Statistically significant difference.)

Enzyme	Strain	Specific activity	*n*	*P*-value (*t*-test)
NADH:Q2	Non	7·7 ± 4·7 U	11	0·653
	Ind	8·8 ± 5·3 U	7	
Complex II (SDH)	Non	41·8 ± 37·4 U	8	0·665
	Ind	34·8 ± 30·6 U	10	
Complex III (bc1)	Non	523 ± 181 mU	18	0·197
	Ind	442 ± 160 mU	14	
Complex IV (COX)	Non	0·83 ± 0·54 mU	7	0·363
	Ind	1·16 ± 0·76 mU	7	
G3PDH	Non	41·2 ± 11·0 mU	8	0·006*
	Ind	60·0 ± 12·2 mU	8	

Mitochondrial fumarate reductase (mtFRD) is an NADH-dependent enzyme catalysing a reaction from fumarate back to succinate. To check whether the NADH:Q2 activity is not masked by a reaction fumarate + NADH → succinate:Q2, a measurement in the presence of 3-methoxy-phenylacetic acid (3-MPA), an inhibitor of mtFRD (Turrens,1989) was performed. In the presence of 3-MPA the overall NADH:Q2 activity was decreased by 10% in both the non-induced and NDH2-depleted cells. Hence, the observed activity cannot be attributed to mtFRD. Since no change in the overall NADH : Q2 oxidoreductase activity occurred, we performed glycerol gradient ultracentrifugation in order to see whether there is a shift in the distribution of this activity. Mitochondria isolated from cells upon induction of RNAi against NDH2 were lysed and layered on top of 10–30% glycerol gradient. Upon centrifugation, fractions were collected from the top. The protein content in each fraction was measured using the Bradford method and the NADH : Q2 activity and its sensitivity to rotenone and DPI were measured. The protein distribution followed the same pattern as shown previously in experiments with complex

https://doi.org/10.1017/S003118201200162X Published online by Cambridge University Press

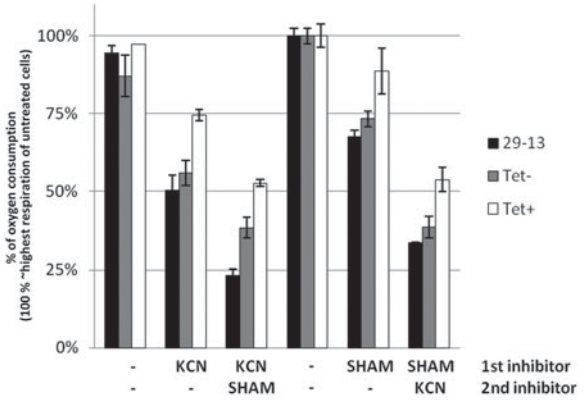

Fig. 4. Analysis of respiration of the NDH2 cells. Respiration of parental (29–13; black columns), non-induced (tet−; grey columns) and RNAi-induced cell lines (tet+; white columns). The highest respiration before the addition of any inhibitor was considered the 100% standard. *x* axis: inhibitor treatment; *y* axis: % of oxygen consumption relative to the highest respiring untreated cells.

I knock-downs (Verner *et al*. 2011). Although there was a distinct difference between the non-induced and induced cells in the distribution of the followed activity and its sensitivity to inhibitors, at present we have no explanation for the observed scattered pattern (Supplementary Online resource 4).

Respiration uses different substrates in NDH2 knock-down

The lack of effect on the NADH dehydrogenase activity led us to measure the overall respiration of the procyclic cells, in which NDH2 was ablated as compared to those with wild-type levels of this protein. While KCN inhibits the cytochrome-mediated pathway by blocking complex IV, SHAM blocks the alternative pathway by interfering with the function of TAO. Measurement from 3 independent non-parallel RNAi inductions was performed. Although overall oxygen consumption showed some variation, the degree of inhibition was consistent throughout the measurements. Upon depletion of NDH2 the sensitivity to KCN and SHAM changed (Fig. 4). Unexpectedly, the fraction of respiration resistant to both KCN and SHAM substantially increased following the depletion of NDH2, regardless of the order in which the drugs were added.

To further investigate the involvement of electron donors in respiration, we prepared digitonin-permeabilized cells and measured oxygen consumption on various substrates upon RNAi induction. The integrity of the mitochondria in the permeabilized cells was checked using DL-glycerol-3-phosphate (G3P) and succinate (SUC). Should the mitochondrial membranes be compromised, the addition of a respiratory substrate would not stimulate oxygen consumption. G3P is processed by mitochondrial glycerol-3-phosphate dehydrogenase located in the mitochondrial inner membrane facing the intermembrane space, while SUC is a substrate of malonate-sensitive respiratory complex II, a protein complex facing the matrix. Both G3P and SUC stimulated respiration sensitive to antimycin A, a specific inhibitor of respiratory complex III, with SUC-stimulated respiration being sensitive also to malonate (data not shown). This way the presence of intact mitochondria with unreleased cytochrome *c* was confirmed.

Next, we evaluated the ability of respiring mitochondria to utilize substrates leading to the formation of NADH. Malate together with pyruvate (MAL+PYR), 2-oxoglutarate (2-OXO), and NADH itself were used. In higher eukaryotes, the combination of MAL+PYR is a source of NADH produced in mitochondrial matrix via the tricarboxylic (TCA) cycle. While the added MAL causes the depletion of TCA intermediates stopping the respiration, PYR will drive TCA. NADH is then produced by the MAL to oxaloacetate reaction; 2 additional NADH molecules are generated between citrate and SUC. Under experimental conditions used, neither MAL alone, nor in combination with PYR (both at 20 mM concentration) stimulated respiration (data not shown). Another substrate, 2-OXO, is converted to SUC with concomitant production of 1 NADH molecule thus supporting both NADH-dependent respiration via complex I and/or NDH2, and succinate-dependent respiration via complex II. In tet− and tet+ cells 6 days of induction, 20 mM 2-OXO stimulated respiration of 0·325 and 0·267 nmol O_2/min/5×10^7 cells, respectively (Table 2). The addition of malonate inhibited the respiration to the same extent (by 60%; data not shown), regardless of RNAi.

Finally, we tested NADH itself as a possible respiratory substrate. In eukaryotes, NADH cannot penetrate the inner mitochondrial membrane and requires a shuttle reaction, such as malate : aspartate to be transported inside of the organelle. However, the presence of an external mitochondrial NADH dehydrogenase, such as the one described in yeasts (Kerscher *et al*. 2002) or plants (Soole and Menz, 1995), leads to respiration on NADH alone. To our surprise, the addition of 10 mM NADH stimulated oxygen consumption in the non-induced cells (1·42 nmol O_2/min/5×10^7 cells). In cells 6 days upon RNAi induction against NDH2, this stimulation was about half as high (0·76 nmol O_2/min/5×10^7 cells). Also, when G3P respiration was quantified, the same elevation as in the previous measurement of the G3PDH activity (4·4 nmol O_2/min/5×10^7 cells and 7·9 nmol O_2/min/5×10^7 cells in tet− and tet+ cells, respectively) was observed.

https://doi.org/10.1017/S003118201200162X Published online by Cambridge University Press

Table 2. Respiration on various substrates of digitonin-permeabilized cells

(Substrate: substrate used for respiration; for concentrations see Materials and Methods section. Induction: non-induced (Non) or RNAi-induced (Ind) cell line; *n*, number of measurements. Absolute respiration: respiration in nmol O_2/l/min/5×10^7 cells, mean and standard deviation; Net: oxygen consumption upon addition of substrate w/o basal oxygen consumption; *P*-value: *P*-value reached using Mann-Whitney non-parametric test, $\alpha=0{\cdot}05$. Relative respiration: relative stimulation of oxygen consumption calculated as (substrate-stimulated respiration/basal respiration) − 1, mean and standard deviation. *Statistically significant difference.)

			Absolute respiration (nmol/min/5×10^7 cells)		Relative respiration	
Substrate	Induction	*n*	Net	*P*-value (M-W)	Stimulation	*P*-value (M-W)
NADH	Non	5	−1·4±0·2	0·003*	1·1±0·5	0·027*
	Ind	5	−0·8±0·2		0·6±0·2	
G3P	Non	3	−4·4±0·3	0·050*	3·2±0·2	0·050*
	Ind	3	−7·9±1·0		6·2±0·9	
2-OXO	Non	2	−0·3±0·0	0·330	0·3±0·1	0·333
	ind	2	−0·4±0·0		0·3±0·0	

DISCUSSION

In this study we performed RNAi-silencing of an alternative rotenone-insensitive NDH2, which is part of the respiratory chain in the procyclic stage of *T. brucei* (Fang and Beattie, 2002). Depletion of NDH2 affected cell growth as well as mitochondrial membrane potential. However, the overall oxygen consumption, ROS production, NADH:Q2 oxidoreductase activity and remaining activities of respiratory complexes were not altered upon the ablation of NDH2, with the sole exception of mitochondrial G3PDH, which was elevated in these cells. The up-regulation of G3PDH was confirmed on digitonin-permeabilized RNAi knock-down cells, when G3P was used as a substrate for respiration. This assay also revealed that NADH can be used as a respiratory substrate, providing evidence for the existence of intermembrane-space oriented NADH:Q oxidoreductase. Decreased NADH-dependent respiration upon RNAi confirms that NDH2 is responsible for this activity.

Although the ablation of NDH2 led to diminished growth, the effect was not lethal, suggesting that either RNAi is not fully efficient or that there is a compensatory activity rescuing the cells and rendering the targeted protein non-essential for cell proliferation. Northern blot analysis confirmed virtually total elimination of the NDH2 mRNA, hence the latter possibility likely takes place. The published results from complex I in both procyclic (Verner *et al*. 2011) and bloodstream cells (Surve *et al*. 2011) showed that, counterintuitively, neither knock-down nor knock-out of complex I subunits led to a growth phenotype. Similar lack of growth phenotype was shown for *T. cruzi* strain with a deletion in maxicircle kinetoplast DNA, rendering complex I inactive (Carranza *et al*. 2009). The presence of a growth phenotype upon RNAi against NDH2, no matter how big it is, contrasts with the lack of phenotype in knock-downs/out of complex I subunits (Surve *et al*. 2011; Verner *et al*. 2011), confirming that in both studied life-cycle stages of *T. brucei*, NDH2 plays a more important role in the metabolism of NADH and maintenance of mitochondrial membrane potential than complex I.

No statistically significant difference was observed for oxygen consumption of intact non-induced and RNAi-induced cells, although a slightly different sensitivity to inhibitors was noted, indicating that there is some kind of compensation taking place in the mitochondrion of RNAi-induced cells. Same lack of effect on oxygen consumption has been observed in cells lacking subunits of complex I (Škodová, I. and Verner, Z., *unpublished data*). However, downregulation of subunits of complexes III and/or IV lead to changes in oxygen consumption and sensitivity to inhibitors of terminal oxidases (Horváth *et al*. 2005; Gnipová *et al*. 2012). Hence, we speculate that the cells are more flexible at the level of entry points of electrons into the respiratory chain and that they can readily redirect metabolism in a way that keeps the number of electrons passing through the system constant. In contrast to electron entry, their exit from the respiratory chain seems to be a critical bottleneck for the system. The existence of a laboratory strain of *Crithidia fasciculata* shown to feed the respiratory chain mainly via complex II, likely rendering complex I dispensable for this monoxenous parasite of insects (Cazzulo, 1992), supports the notion that there is a substantial metabolic flexibility upstream of ubiquinone. However, studies performed with *T. brucei* showed that the situation is rather different in this flagellate. While complex II is non-essential for the procyclic stage grown on glucose (Coustou *et al*. 2008), it is complex I that is dispensable, yet still active in these cells (Verner *et al*. 2011). A different situation evolved in *P. serpens*, which lost all

https://doi.org/10.1017/S003118201200162X Published online by Cambridge University Press

mitochondrial- (Nawathean and Maslov, 2000) and at least some nuclear-encoded subunits of respiratory complexes III and IV (Maslov *et al*. 2002). Therefore, this plant parasite relies on complex I, which is the only remaining classical proton pump, with complex V as the site of ATP synthesis (Čermáková *et al*. 2007).

Mitochondrial membrane potential and the level of ROS production depend on a functional respiratory chain. In general, the potential across the inner membrane is generated by complexes I, III and IV, with ROS being formed by electrons leaking from the respiratory chain to oxygen at places other than terminal oxidases, usually at complexes I and/or III (Brand, 2010). In *T. brucei*, complex I was shown to be present yet it does not to influence any of these features (Surve *et al*. 2011; Verner *et al*. 2011). Interestingly, membrane potential was decreased as a consequence of NDH2 RNAi. Since NDH2 does not have the capacity to translocate protons across the inner mitochondrial membrane, the observed effect is likely triggered downstream of ubiquinone. Fewer electrons passing through complexes III and IV would be consistent with lower mitochondrial membrane potential. Since the ablation of NDH2 did not change overall oxygen consumption, and membrane potential droped, the electrons need to be channelled to TAO. Unaltered ROS production in cells depleted for NDH2 is consistent with the observation by Gnipová *et al*. (2012) who showed that an increase in ROS production corresponds to an increase in complex III activity. In our case, the activity of complex III remained constant, the same as the production of ROS.

After we had checked the *in vivo* parameters of the NDH2-depleted cells, we tested the *in vitro* activities of enzymes involved in electron transfer in the respiratory chain. None of the measured enzymes showed altered activity with the exception of mitochondrial FAD-dependent G3PDH. In the bloodstream stage, this dehydrogenase is responsible for oxygen consumption with electrons being shuffled via ubiquinone to TAO, a terminal oxidase not contributing to membrane potential (Clarkson *et al*. 1989). Although direct proof is missing, unaltered oxygen consumption and lower membrane potential suggest that the pathway may be working the same way in the procyclic stage, at least under the conditions of NDH2 depletion. Moreover, unaltered activities of complexes III and IV confirm that the observed decrease of membrane potential is not due to their inability to process electrons, but is instead caused by the lower number of electrons passing through these complexes. Surprisingly, silencing of complex I caused only a mild 20% decrease of the NADH : Q2 activity (Verner *et al*. 2011), with respiratory complexes II through IV unchanged (Škodová, I. and Dunajčíková-Čermáková, P., *unpublished data*). Moreover, Surve *et al*. (2011) reported no decrease of NADH : Q2 activity in lysates prepared from knock-out cells for subunits of complex I, as compared to the parental cells. Therefore, at least 80% of the measured NADH : Q2 activity is to be attributed to another NADH : Q2 dehydrogenase and not complex I/NDH2. We can only hypothesize that Q2 may not be the best acceptor for assaying NDH2 activity. Overall, acceptors with lower redox potential, such as ferricyanide or 2,6-dichlorophenoindophenol gave much higher NADH dehydrogenase activities (Čermáková, P. and Verner, Z., *unpublished data*). On the other hand, the lower redox potential of these acceptors leads to an increased number of interfering reactions rendering these acceptors practically inapplicable unless the isolated enzyme could be characterized. Interestingly, Q2 is readily used by mitochondrial lysates of *P. serpens*, a kinetoplastid flagellate with active complex I sensitive to its classical inhibitor rotenone (Čermáková *et al*. 2007). The current study also shows an urgent need for a functional approach in descriptive biochemistry. Fang and Beattie (2002) identified NDH2 and, using a recombinant protein, performed NADH dehydrogenase activity assays with a limited set of ubiquinone derivatives, namely duroquinone, and ubiquinones Q0 and Q1. Since all Q-species used are mere derivatives of the naturally occurring hydrophobic ubiquinones Q9/Q10, the possibility that *in vivo* activities are substantially different from the *in vitro* ones cannot be excluded.

In a previous study, we performed a glycerol gradient sedimentation of mitochondrial lysates prepared from cell lines depleted for subunits of complex I (Verner *et al*. 2011). Upon RNAi, we observed a different pattern in sedimentation of NADH : Q2 activity and its sensitivity to complex I inhibitor, rotenone, and a general flavin-enzyme inhibitor, DPI. We concluded that the overall low decrease of NADH : Q2 activity is due to an up-regulation of a different flavine enzyme (Verner *et al*. 2011). The same analysis was performed in cells ablated for NDH2; however, the results were not consistent with data obtained from complex I. Hence, the data are compatible with a scenario, according to which in complex I knock-downs, an enzyme different from NDH2 became upregulated. Conversely, silencing of NDH2 did not influence complex I. Also, this observation further supports a hypothesis of Q2 not being used by NDH2 as an electron acceptor.

The final experiment confirming involvement of NDH2 in the respiratory chain has been the respiration of digitonin-permeabilized cells on different substrates, which showed elevated mitochondrial G3PDH as well as unaltered activity of complex II. Strikingly, the addition of NADH alone triggered oxygen consumption by the non-induced cells that was lower in the RNAi cells. Moreover, this experiment allows the position of NDH2 in the membrane to be addressed. So far, in metabolic pathways,

https://doi.org/10.1017/S003118201200162X Published online by Cambridge University Press

NDH2 was depicted as an alternative to complex I facing the matrix side of the mitochondrial inner membrane (Coustou *et al*. 2008; Ebikeme *et al*. 2010; Tielens and Hellemond, 2009). The most important conclusion of this experiment is based on the well-known impermeability of the inner mitochondrial membrane to NADH. In general, to be able to re-oxidize cytosolic NADH the cell employs shuttles to transport this reduced co-factor into the mitochondrial matrix. The commonly known malateaspartate shuttle requires a source of intramitochondrial aspartate and extramitochondrial malate. Given the way the digitonin-permeabilized cells were prepared, together with the lack of respiration on malate alone, we can be sure that there is not enough endogenous substrate for a shuttle transport of NADH into the mitochondrial matrix. Thus, the stimulation of respiration by NADH is possible only if the NDH2 faces intermembrane space and not mitochondrial matrix. This situation is in agreement with the position of NDH2 in some yeasts (Kerscher *et al*. 2002) and plants (Soole and Menz, 1995).

The substrate 2-oxoglutarate, used as one of the respiratory substrates, is metabolized to succinate through succinyl-CoA with concomitant production of NADH inside the mitochondrial matrix. Respiration using this substrate was sensitive to malonate, a competitive inhibitor of complex II, further implicating this complex with the respiration on 2-oxoglutarate. Moreover, malonate inhibited respiration to the same extent in both non- and induced cells, suggesting that the processing of NADH inside mitochondrial matrix is not altered upon RNAi; this further confirms the directional facing of NDH2 into the intermembrane space. The inability of malate and pyruvate to stimulate respiration confirms previous reports on TCA not running as a regular cycle (van Weelden *et al*. 2005). Acetyl-CoA produced from pyruvate by the pyruvate dehydrogenase complex is metabolized to acetate via acetatesuccinate CoA transferase, generating ATP via substrate level phosphorylation (Riviére *et al*. 2004). Alternatively, acetyl-CoA might be metabolized by a branch leading to beta-hydroxybutyrate, yet none of these pathways generate respiration substrate(s). Combination of malate with pyruvate is used to enable malate transport into the mitochondrion of typical eukaryotes. However, with pyruvate not being used by TCA, malate might not be able to enter the mitochondrion of *T. brucei*. Its import is dependent on di- and tricarboxylate carriers that exchange malate for either H_3PO_4 or citrate/isocitrate with concomitant proton transport (tricarboxylate carrier). Alternatively, malate could be transported by 2-oxoglutarate carrier in exchange for 2-oxoglutarate (Gneiger, 2011). With pyruvate not entering TCA, the source of exchangeable intermediates is not present.

ACKNOWLEDGEMENTS

We thank Petra Čermáková and Eva Kriegová for help with some experiments and Ivan Hrdý for stimulating discussions on electron transport chain of *T. brucei* and other odd eukaryotes. Last but not least, we thank Hassan Hashimi for reading of the manuscript.

FINANCIAL SUPPORT

This work was supported by the Grant Agency of the Czech Republic 204/09/1667, the Czech Ministry of Education (LC07032 and 6007665801), and the Praemium Academiae award to J. L., who is a Fellow of the Canadian Institute of Advanced Research, and by the Scientific Grant Agency of the Slovak Ministry of Education and the Academy of Sciences 1/0393/09. Final experiments were supported by The National Scholarship Programme of the Slovak Republic for the Support of Mobility of Students, Ph.D. Students, University Teachers, Researchers and Artists.

REFERENCES

Brand, M. D. (2010). The sites and topology of mitochondrial superoxide production. *Experimental Gerontology* **45**, 466–472. doi: 10.1016/j.exger.2010.01.003.

Carranza, J. C., Kowaltowski, A. J., Mendonça, M. A. G., de Oliveira, T. C., Gadelha, F. R. and Zingales, B. (2009). Mitochondrial bioenergetics and redox state are unaltered in *Trypanosoma cruzi* isolates with compromised mitochondrial complex I subunit genes. *Journal of Bioenergetics and Biomembranes* **41**, 299–308. doi: 10.1007/s10863-009-9228-4.

Cazzulo, J. J. (1992). Aerobic fermentation of glucose by trypanosomatids. *The FASEB Journal* **6**, 3153–3161.

Čermáková, P., Verner, Z., Man, P., Lukeš, J. and Horváth, A. (2007). Characterization of the NADH:ubiquinone oxidoreductase (complex I) in the trypanosomatid *Phytomonas serpens* (Kinetoplastida). *The FEBS Journal* **274**, 3150–3158. doi: 10.1111/j.1742-4658.2007.05847.x.

Chaudhuri, M., Ajayi, W., Temples, S. and Hill, G. C. (1995). Identification and partial purification of a stage-specific 33 kDa mitochondrial protein as the alternative oxidase of the *Trypanosoma brucei brucei* bloodstream trypomastigotes. *The Journal of Eukaryotic Microbiology* **42**, 467–472. doi: 10.1111/j.1550-7408.1995.tb05892.x.

Clarkson, A. B., Jr, Bienen, E. J., Pollakis, G. and Grady, R. W. (1989). Respiration of bloodstream forms of the parasite *Trypanosoma brucei brucei* is dependent on a a plant-like alternative oxidase. *The Journal of Biological Chemistry* **264**, 17770–17776.

Coustou, V., Biran, M., Breton, M., Guegan, F., Riviére, L., Plazzoles, N., Nolan, D., Barret, M. P., Franconi, J. M. and Bringaud, F. (2008). Glucose-induced remodeling of intermediary and energy metabolism in procyclic *Trypanosoma brucei*. *The Journal of Biological Chemistry* **283**, 16342–16354. doi: 10.1074/jbc.M709592200.

Ebikeme, C., Hubert, J., Biran, M., Gouspillou, G., Morand, P., Plazolles, N., Guegan, F., Diolez, P., Franconi, J.-M., Portais, J.-C. and Bringaud, F. (2010). Ablation of succinate production from glucose metabolism in the procyclic trypanosomes induces metabolic switches to the glycerol 3-phosphate/dihydroxyacetone phosphate shuttle and to proline metabolism. *The Journal of Biological Chemistry* **285**, 32312–32324. doi: 10.1074/jbc.M110.124917.

Fang, J. and Beattie, D. S. (2002). Novel FMN-containing rotenone-insensitive NADH dehydrogenase from *Trypanosoma brucei* mitochondria: isolation and characterization. *Biochemistry* **41**, 3065–3072. doi: 10.1021/bi015989w.

Fang, J. and Beattie, D. S. (2003). Identification of a gene encoding a 54 kDa alternative NADH dehydrogenase in *Trypanosoma brucei*. *Molecular and Biochemical Parasitology* **127**, 73–77. doi: 10.1016/S0166-6851(02)00305-5.

Galkin, A. and Brandt, U. (2005). Superoxide radical formation by pure complex I (NADH: Ubiquinone oxidoreductase) from *Yarrowia lipolytica*. *The Journal of Biological Chemistry* **280**, 30129–30135. doi: 10.1074/jbc.M504709200.

Gneiger, E. (2011). Mitochondrial Pathways and Respiratory Control. 2nd Edn. OROBOROS MiPNet Publications, Innsbruck, Austria.

Gnipová, A., Panicucci, B., Paris, Z., Verner, Z., Horváth, A., Lukeš, J. and Zíková, A. (2012). Disparate phenotypic effects from the knockdown of

various *Trypanosoma brucei* cytochrome c oxidase subunits. *Molecular and Biochemical Parasitology* **184**, 90–98. doi: 10.1016/j.molbiopara.2012.04.013.

Guerra, D. G., Decottignies, A., Bakker, B. M. and Michels, P. A. M. (2006). The mitochondrial FAD-dependent glycerol-3-phosphate dehydrogenase of Trypanosomatidae and the glycosomal redox balance of insect stages of *Trypanosoma brucei* and *Leishmania* spp. *Molecular and Biochemical Parasitology* **149**, 155–169. doi: 10.1016/j.molbiopara.2006.05.006.

Hashimi, H., Zíková, A., Panigrahi, A. K., Stuart, K. D. and Lukeš, J. (2008). TbRGG1, an essential protein involved in kinetoplastid RNA metabolism that is associated with a novel multiprotein complex. *RNA* **14**, 970–980. doi: 10.1261/rna.888808.

Horváth, A., Horáková, E., Dunajčíková, P., Verner, Z., Pravdová, E., Šlapetová, I., Cuninková, L. and Lukeš, J. (2005). Downregulation of the nuclear-encoded subunits of the complexes III and IV disrupts their respective complexes but not complex I in procyclic *Trypanosoma brucei*. *Molecular Microbiology* **58**, 116–130. doi: 10.1111/j.1365-2958.2005.04813.x.

Kerscher, S., Dröse, S., Zwicker, K., Zickermann, V. and Brandt, U. (2002) *Yarrowia lipolytica*, a yeast genetic system to study mitochondrial complex I. *Biochimica et Biophysica Acta* **1555**, 83–91. doi: 10.1016/S0005-2728(02)00259-1.

Maslov, D. A., Zíková, A., Kyselová, I. and Lukeš, J. (2002). A putative novel nuclear-encoded subunit of the cytochrome *c* oxidase complex in trypanosomatids. *Molecular and Biochemical Parasitology* **125**, 113–125. doi: 10.1016/S0166-6851(02)00235-9.

Nawathean, P. and Maslov, D. A. (2000). The absence of genes for cytochrome *c* oxidase and reductase subunits in maxicircle kinetoplast DNA of the respiration-deficient plant trypanosomatid *Phytomonas serpens*. *Current Genetics* **38**, 95–103. doi: 10.1007/s002940000135.

Ott, M., Gogvadze, V., Orrenius, S. and Zhivotovsky, B. (2007). Mitochondria, oxidative stress and cell death. *Apoptosis* **12**, 913–922. doi: 10.1007/s10495-007-0756-2.

Riviére, L., van Weelden, S. W., Glass, P., Vegh, P., Coustou, V., Biran, M., van Hellemond, J. J., Bringaud, F., Tielens, A. G. and Boshart, M. (2004). Acetyl:succinate CoA-transferase in procyclic *Trypanosoma brucei*. Gene identification and role in carbohydrate metabolism. *The Journal of Biological Chemistry* **279**, 45337–45346. doi: 10.1074/jbc.M407513200.

Soole, K. L. and Menz, R. I. (1995). Functional molecular aspects of the NADH dehydrogenases of plant mitochnondria. *Journal of Bioenergetics and Biomembranes* **27**, 397–406. doi: 10.1007/BF02110002.

Surve, S., Heestand, M., Panicucci, B., Schnaufer, A. and Parsons, M. (2011). Enigmatic presence of mitochondrial complex I in *Trypanosoma brucei* bloodstream forms. *Eukaryotic Cell* **11**, 183–193. doi: 10.1128/EC.05282-11.

Tielens, A. G. M. and van Hellemond, J. J. (2009). Surprising variety in energy metabolism within Trypanosomatidae. *Trends in Parasitology* **25**, 482–490. doi:10.1016/j.pt.2009.07.007.

Turrens, J. F. (1989). The role of succinate in the respiratory chain of *Trypanosoma brucei* procyclic trypomastigotes. *Biochemical Journal* **259**, 363–368.

Verner, Z., Čermáková, P., Škodová, I., Kriegová, E., Horváth, A. and Lukeš, J. (2011). Complex I (NADH:ubiquinone oxidoreductase) is active in but non-essential for procyclic *Trypanosoma brucei*. *Molecular and Biochemical Parasitology* **175**, 196–200. doi: 10.1016/j.molbiopara.2010.11.003.

Vondrušková, E., van den Burg, J., Zíková, A., Ernst, N. L., Stuart, K., Benne, R. and Lukeš, J. (2005). RNA Interference analyses suggest a transcript-specific regulatory role for mitochondrial RNA-binding proteins MRP1 and MRP2 in RNA editing and other RNA processing in *Trypanosoma brucei*. *The Journal of Biological Chemistry* **280**, 2429–2438. doi: 10.1074/jbc.M405933200.

van Weelden, S. W., van Hellemond, J. J., Opperdoes, F. R. and Tielens, A. G. (2005). New functions for parts of the Krebs cycle in procyclic *Trypanosoma brucei*, a cycle not operating as a cycle. *The Journal of Biological Chemistry* **280**, 12451–12460. doi: 10.1074/jbc.M412447200.

Wickstead, B., Ersfeld, K. and Gull, K. (2002). Targeting of a tetracycline-inducible expression system to the transcriptionally silent minichromosomes of *Trypanosoma brucei*. *Molecular and Biochemical Parasitology* **125**, 211–216. doi: 10.1016/S0166-6851(02)00238-4.